J. Physiol. (1976), **255**, *pp.* 105–135
With 1 plate and 13 text-figures
Printed in Great Britain

THE IONIC BASIS OF THE RESTING POTENTIAL AND A SLOW DEPOLARIZING RESPONSE IN ROHON-BEARD NEURONES OF *XENOPUS* TADPOLES

BY N. C. SPITZER

From the Department of Biology, University of California, San Diego, La Jolla, California 92093, U.S.A.

(*Received 19 May 1975*)

SUMMARY

1. Rohon–Beard cells in the spinal cord of *Xenopus laevis* tadpoles have been studied in animals 4-days to 2-weeks-old (Nieuwkoop & Faber, 1956, stages 45–49). These neurones have an unusually large resting membrane potential of −88 mV, in Ringer solution containing 3·0 mM K^+.

2. Their resting potential (R.P.) depends on the concentration gradient of K^+ across the cell membrane. These cells follow the prediction of the Nernst equation for a K^+-selective electrode, down to external K^+ concentrations as low as 1·0 mM (R.P. −118 mV).

3. The resting potentials of muscle cells in these animals exhibit the same dependence on external [K^+], as has been shown previously.

4. Rohon–Beard cells can be driven antidromically, by stimulation of the anterior end of the spinal cord with brief current pulses through a suction electrode. Antidromic action potentials fail to invade the cell body with repeated stimulation at 1 Hz.

5. Even when impulses fail to invade Rohon–Beard somata, slow depolarizations can be produced by single shocks or trains of shocks which cause impulse activity in other neurones. The response can be observed to a single stimulus or to a train of stimuli. The magnitude of the depolarization is graded, depending on the number of stimuli and the frequency of stimulation.

6. Support is presented for the hypothesis that the slow depolarization in Rohon–Beard cells is mediated by the release of K^+ into their environment by the impulse activity of neighbouring neurones. The slow depolarization increases in solutions containing 1·5 mM-K^+, and decreases in solutions containing 6·0 mM-K^+. The changes are in quantitative agreement with those anticipated by theory.

7. The slow depolarization is unlikely to be due to a conductance

change produced by a synaptic transmitter, since hyperpolarization and depolarization of the Rohon–Beard cell with injected current do not change the amplitude of the response. Further, low Ca–high Mg solutions which block neuromuscular transmission do not block the response.

8. The possible role of the slow depolarizing response in the physiological activity of these neurones is discussed.

INTRODUCTION

The normal resting potentials of most cells arise as diffusion potentials of potassium, sodium and other ions to which the membrane is permeable. It has been shown that glial cells have resting potentials that depend exclusively on the concentration ratio of potassium inside to potassium outside, in the physiological range of concentrations (Kuffler, Nicholls & Orkand, 1966). These glia thus behave like K^+ electrodes, and their potentials are accurately predicted by the Nernst equation, down to $[K^+]_o$ of 1·5 m-mole/l. Some muscle cells also have resting potentials that are at the K equilibrium potential (E_K), down to low extracellular concentrations of K^+ (Kernan, 1960; Cohen, Gerschenfeld & Kuffler, 1968).

By contrast, in nerve cells the resting potential generally does not follow the prediction of the Nernst equation. At low external K^+ concentrations the potentials are less negative inside than those expected from theory, because the resting conductance to other ions (notably Na^+ and Cl^-) is appreciable (Huxley & Stämpfli, 1951). Neuronal resting potentials can be predicted by the Goldman equation, which takes into account the membrane permeability to these other ions.

In the course of an investigation of the properties of Rohon–Beard neurones in the spinal cord of amphibian tadpoles, I noticed that these cells had unusually large resting potentials. A systematic examination of the ionic dependence of their potentials has revealed that they behave like good K^+ electrodes. Their resting potential, like that of glia, agrees with the value expected from the Nernst equation, down to $[K^+]_o$ of 1·0 m-mole/l. Muscle cells in these tadpoles have fully comparable resting potentials through the same range of external K^+ concentrations.

The inward Na current of a neuronal action potential is followed by an outward potassium current, which causes the repolarization of the cell. The efflux of K^+ resulting from these electrical signals increases the extracellular K^+ concentration locally for brief periods, shifting E_K to more positive values. Orkand, Nicholls & Kuffler (1966) showed that impulses in amphibian optic nerves caused a slow depolarization of the surrounding glial cells by this mechanism. The undershoot following an action potential occurs because the K^+ conductance dominates the others and the

membrane potential is driven toward E_K. Frankenhaeuser & Hodgkin (1956) and Baylor & Nicholls (1969*a*) observed that the increase in $[K^+]_o$ following impulse activity in squid axons and leech neurones caused a decrease in the size of their undershoot, by the same mechanism. It was further shown that spontaneous firing patterns and synaptic potentials were affected by the build-up of extracellular K. I will show that impulse activity of neurones in the spinal cord causes a change in the resting potential of Rohon–Beard neurones; the cells are depolarized in a manner consistent with the local accumulation of extracellular K^+, like glia.

METHODS

Rohon–Beard cells were first described in the late 1800s by Freud (1877), Rohon (1885), and Beard (1889). They are seen in the dorsal region of the spinal cord, early in the development of lamprey, elasmobranch, teleost and amphibian embryos. Their location, staining properties, and the demonstration of processes running to the periphery and in the spinal cord led to their classification as neurones. The work of Coghill (1914) and DuShane (1938), on embryos of the salamander, *Ambystoma*, led to the conclusion that the cells serve a sensory function and are the afferent limb of a three neurone reflex arc. Hughes (1957) showed that there are roughly 150 Rohon–Beard cells in *Xenopus* embryos; they send processes out to the periphery and other fibres longitudinally in the spinal cord. He documented their distribution in the cord and migration from the lateral margins to the mid line during development of the tadpole.

Rovainen (1967) has studied the dorsal cells of the lamprey with intracellular micro-electrodes; these neurones are thought to be homologous with amphibian Rohon–Beard cells. Martin & Wickelgren (1971) have demonstrated that the dorsal cells are primary sensory neurones. No other electrophysiological investigation of these cells has appeared.

Animals

Pairs of male and female adult *Xenopus laevis* were maintained in tap water in separate tanks at room temperature (21° C) and fed weekly with a mixture of chopped beef heart and cod liver oil. A pair was mated as frequently as once a month; breeding was induced by a primer injection of 100 i.u. of human chorionic gonadotropin (Sigma) to both animals, followed by an equal dose a day later. Animals were left in a darkened tank and fertilized eggs were usually obtained within 24 hr (yield 50 to $\sim$1000).

Embryos were raised in 10 % Holtfreter's solution; they developed in accordance with the normal timetable established by Nieuwkoop & Faber (1956). The solution was never changed for any batch of tadpoles, though the depth in the tank was increased from one inch to 4–5 in. after hatching, and the population was thinned out to prevent any high density inhibition of growth rate and development. When the mouth broke through, the tadpoles were fed daily with a few drops of an aqueous solution of commercially available powdered yeast (Fleischmann's). A few animals were carried through metamorphosis (2½ months). Most of the experiments reported here were made on animals 4–14 days old (Nieuwkoop & Faber, 1956 stages 45–49).

Preparations

The tadpoles are 8–20 mm in length; dissections were accomplished with the variable magnification (up to × 60) of a Wild M7 zoom stereo dissecting microscope. Tadpoles were chilled for temporary anaesthesia and then immobilized by transection of the spinal cord at the level of the fifth myotome; subsequent operations were carried out at room temperature. The dorsal and ventral fins were cut away with irridectomy scissors, the skin pulled back off the trunk musculature and removed, and the cephalo-thorax anterior to the initial cut was discarded. The muscle and pigment cells overlying the spinal cord were removed, using jewellers' forceps and electrolytically sharpened tungsten needles. The preparation consists of the exposed spinal cord, overlying the notochord, with the myotomes of the trunk on either side.

The preparation chamber was a 50 mm plastic Petri dish with a thin glass coverslip cemented under a $\frac{1}{2}$ in. hole in the bottom. The tadpole lay in a long thin slit cut from a thin layer of clear plastic resin (Sylgard) on the bottom of the dish, directly above the coverglass, and was held down by a pair of fine stainless-steel Minuten pins, running through the musculature at either end of the animal and into the Sylgard.

The chamber was mounted on the stage of a compound microscope for electrophysiological experiments. Rohon–Beard neurones in the spinal cord, muscle cells and dorsal root ganglia were viewed directly with Zeiss–Nomarski interference contrast optics using 12·5 × oculars and a 40 × water immersion lens (McMahan & Kuffler, 1971).

Recording conditions

Satisfactory impalements of cells were obtained under visual control with high impedance glass capillary micro-electrodes, fibre filled with 3 M-K acetate (90–180 MΩ). The reference bath electrode consisted of a capillary with a large tip, filled with 3 M-KCl in agar. Tests showed that changing solutions caused less than 2 mV change in the potential recorded between the two electrodes when both were extracellular. Voltages were led off to a cathode follower amplifier with capacitance compensation and current injection capability (WP Instruments – M4A), and displayed on an oscilloscope, often at several gains simultaneously. Cells could often be penetrated by tapping the micromanipulator in a conventional fashion, but best intracellular recordings were obtained, particularly from muscle cells, using brief capacitance overcompensation after dimpling the cell membrane with the electrode. Cells could occasionally be held for up to an hour. Resting membrane potentials were recorded to an accuracy of 1 mV by backing off the recorded voltage with a calibrator located between the bath and ground.

When determining the value of the resting potential in Ringer of different K^+ concentrations, the perfusion solution was changed from standard (4·3 mM) to some altered value (ΔK^+) and back to standard. Resting potential values were accepted when the two determinations in normal Ringer differed by less than 3 mV. Further requirements were that the electrode resistance had not changed by more than 15 MΩ during the measurement, that the zero reference potential on exit was within 2 mV of that on entry, and that the tip potential was ≤ 5 mV, ascertained by breaking the electrode tip. When these criteria were satisfied the results were very repeatable.

Cells were depolarized or hyperpolarized with small currents passed through the recording electrode. In some experiments the spinal cord was stimulated with a suction electrode mounted on the chamber and applied to the anterior end of the cord. The changes in cell membrane potentials in response to stimulation were

differentiated on line with an active circuit with a time constant of 10 msec, and displayed on the oscilloscope; the circuit has a linear output to sine wave input only from 100 to 1000 Hz.

The preparation survived well for periods up to 10 hr; all experiments were made at 22° C.

Solutions

The Standard Ringer solution had the following composition (m-mole/l.): NaCl, 110·7; KCl, 4·3; $CaCl_2$, 1·0; $MgCl_2$, 0·6; $MgSO_4$, 0·8; glucose, 8·0. It was buffered at pH 7·4 with 5·0 mM Tris-maleate. An additional 10·0 mM-$CaCl_2$ was added to promote more stable impalements. In experiments involving changes in $[K^+]$, sulphate salts replaced the chloride salts, to avoid swelling of the cells due to movements of KCl. Dicationic salts (e.g. Na_2SO_4) were used at half the above molarities, and the tonicity was balanced by the addition of sucrose. $CaSO_4$ is only sparingly soluble in water but stirring overnight brought much more of it into solution. Changes in $[K^+]$ were compensated by corresponding changes in $[Na^+]$. When the spinal cord was stimulated, (+)tubocurarine, 10^{-5} g/ml. (Calbiochem) was added to solutions to block muscular contraction.

The preparation was continuously perfused. Fine polyethylene tubing delivered Ringer solution to the anterior end of the preparation and removed it from the posterior end. Different reservoirs could be connected to the inflow line with the turn of a tap. The chamber volume was 0·5 ml. and the flow rate 7 ml./min; when $[K^+]$ was changed the membrane potential shifted briskly, reaching 90 % of its new value in 15 sec.

Anatomy

Animals were fixed in phosphate-buffered 1 % OsO_4 and embedded in Epon. Half micron sections were cut with a glass knife, stained with 1 % toluidine blue and examined with Nomarski optics.

RESULTS

Visualization of Rohon–Beard neurones

The visualization of the preparation with Nomarski optics is illustrated in Pl. 1, fig. 1. Looking down on the dorsal surface of the spinal cord of a stage 48 tadpole, three Rohon–Beard cell bodies are seen in the mid line, almost 25 μm in diameter. The large nucleus, prominent nucleolus, and cell processes extending anteriorly and posteriorly are characteristic of these cells. Other cell processes course along the surface of the cord on either side; the faint outlines of the cell bodies of other, smaller neurones are visible beneath these fibres. The dissection leaves as many as twenty-five cells intact and accessible to impalement with an intracellular microelectrode.

The identification of these cells as Rohon–Beard neurones is based at present on the following criteria: (1) they are relatively large – larger than other cells in the cord; (2) they are located superficially, on the surface of the cord; (3) at early stages they occupy lateral positions on either side of the cord, and migrate into the mid line during the course of

development. The big nucleolus often permits recognition of a cell when the outline of the cell body is not well defined.

A transverse section through the spinal cord of a fixed and embedded tadpole at stage NF 42 is shown in Pl. 1, fig. 2 (micrograph kindly provided by J. Spitzer). A Rohon–Beard cell is seen in cross-section at the top of the cord. At this stage cellular inclusions of yolk granules and lipid droplets make visualization of cell bodies *in vivo* more difficult.

Action potentials

An important criterion for the identification of these cells as neurones and not glia is their ability to fire an action potential in response to depolarizing currents. The response to a brief current pulse delivered through the intracellular recording electrode is seen in Text-fig. 1. Passive depolarization occurs in response to a subthreshold stimulus, and when the current is sufficiently large, an all-or-none regenerative response is seen after the termination of the current pulse. The peak of the action potential overshoots zero by 20 mV; the spike has a duration of 0·5 msec where it crosses the zero potential. There is no undershoot following the down stroke of repolarization.

An action potential is also produced in response to longer current pulses. Threshold currents cause depolarization with marked delayed rectification in 50 % of trials, and give rise to an action potential in 50 %. The differentiated voltage record (dV/dt) indicates a maximum rate of rise of more than 200 V/sec. The ionic basis of the action potential will be discussed elsewhere.

The input resistance (R_{IN}) for this cell (1*C*, *D*) is 37 MΩ. The major and minor axes of this cell, measured *in vivo* with an ocular micrometer, were 31 and 28 μm. The prolate spheroid generated by the rotation of this ellipse has a surface area of 2634 μm^2, a reasonable approximation to the cell membrane area. If the processes are ignored the specific resistance (R_m) of the cell is 975 $\Omega\ cm^2$.

Resting potentials in Rohon–Beard neurones

The membrane potential of Rohon–Beard cells in 4·3 mM $[K^+]_o$ was observed to be close to −80 mV when completely satisfactory, stable impalements were obtained. This large value prompted detailed study of the ionic dependence of the resting potential. The mean resting potential ranged from −53 mV in 12·0 mM $[K^+]_o$ to −118 mV in 1·0 mM, and down to −131 mV in 0·3 mM. A concentration of 18·0 mM $[K^+]_o$ produced twitching of muscle cells, making measurements of resting potentials difficult. These results are presented in Text-fig. 2, in which the magnitude of the resting potential is plotted against log $[K^+]_o$. Each point indicates the mean ± S.E. for the number of cells shown in parentheses, and the line

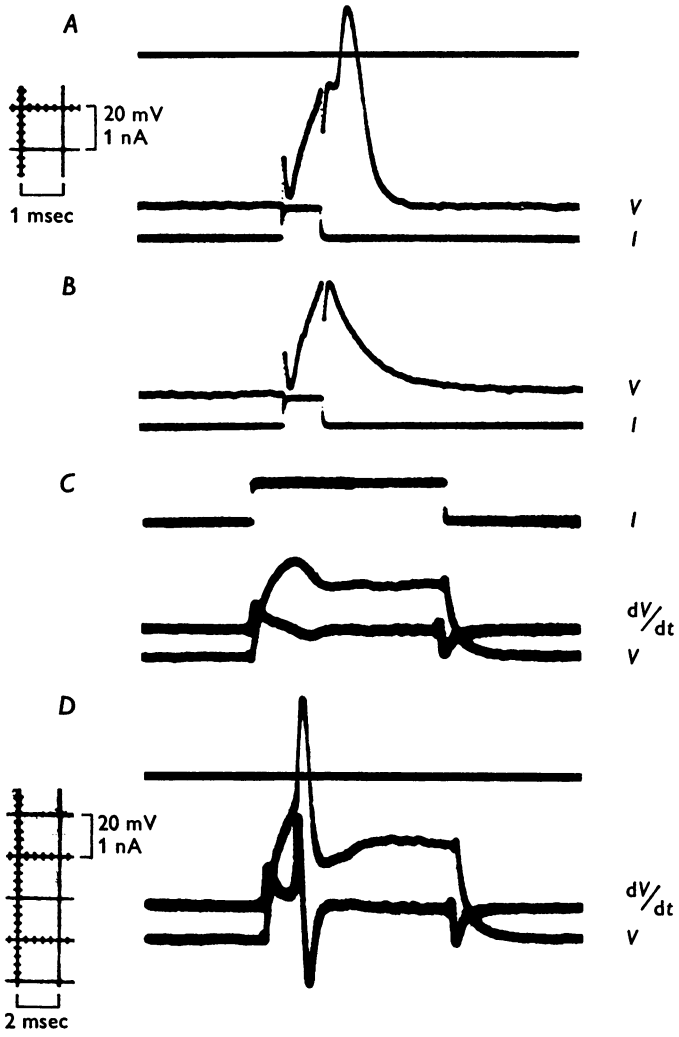

Text-fig. 1. Action potential in a Rohon–Beard neurone, in response to a brief depolarizing current pulse delivered through the intracellular recording electrode. *A*, the threshold current elicits a regenerative response. The absence of an undershoot is characteristic of the spikes produced in this fashion. *B*, the same current fails to elicit more than passive depolarization of the cell. *A*, *B*: resting potential -75 mV (4·3 mM $[K^+]_o$); stage NF 49. *C*, subthreshold stimulation depolarizes the cell; initial hump indicates delayed rectification. *D*, the current produces a spike; rate of rise and fall indicated by dV/dt record. *C*, *D*: resting potential -78 mV (4·3 mM $[K^+]_o$), NF 47.

through the points was drawn by eye. The slope of this semilog plot between 12·0 and 1·0 mM is 59·5 mV per decade change in the concentration of K_o^+. From the Nernst equation, a transmembrane potential determined only by diffusion of K^+ is

$$E_K = \frac{RT}{nF} \ln \frac{[K^+]_o}{[K^+]_i} = 58{\cdot}5 \log \frac{[K^+]_o}{[K^+]_i} \text{ at } 22° \text{ C.}$$

A good K^+ electrode thus shows nearly a 59 mV shift for a tenfold change in the K^+ concentration ratio. In the range of concentrations indicated,

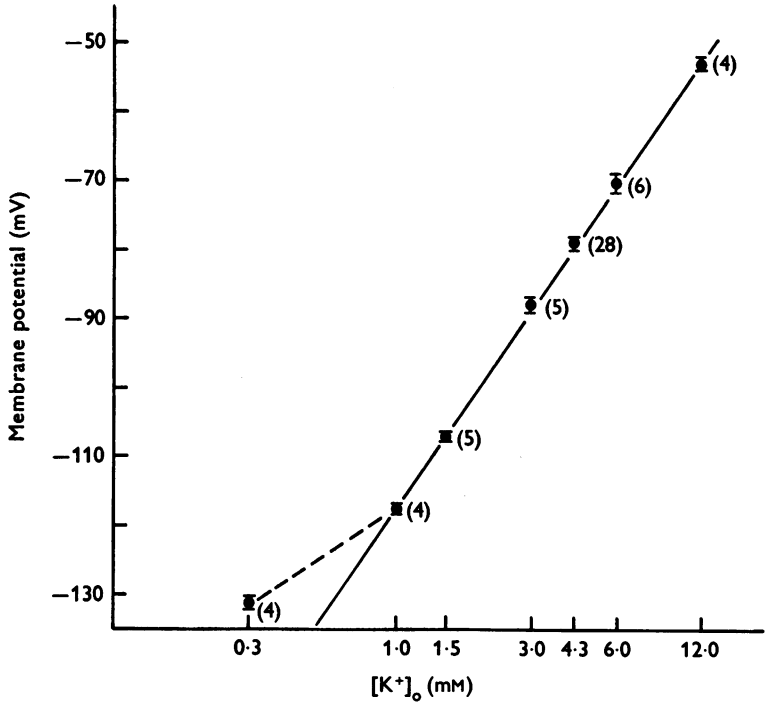

Text-fig. 2. Relation between the Rohon–Beard neurone resting membrane potential and K^+ concentration in Ringer solution, on a semi-logarithmic plot. Each point is the mean ± S.E. for the number of cells indicated in parentheses. The lines through the points were drawn by eye. The continuous line has a slope of 59·5 mV for a tenfold change in $[K^+]_o$. The $[K^+]_i$ is calculated to be 99 m-mole/l. NF 45–49.

this evidence strongly suggests that the Rohon–Beard neurones (NF 45–49) have resting potentials which depend wholly on the ratio of K^+ concentrations on either side of the membrane. Calculation shows the mean internal concentration of K^+ is 99 mM.

Below 1·0 mM-$[K^+]_o$ there is some deviation from the prediction of the Nernst equation, indicated by the dashed line in Text-fig. 2. The resting

potential in 0·3 mM-$[K^+]_o$ is only -131 mV, presumably because the contribution of the resting membrane permeability to Na^+ becomes significant. It would be expected that the resting potential would then be given by the Goldman equation:

$$E_M = \frac{RT}{F} \ln \frac{P_K[K^+]_o + P_{Na}[Na^+]_o + P_{Cl}[Cl^-]_i}{P_K[K^+]_i + P_{Na}[Na^+]_i + P_{Cl}[Cl^-]_o}$$

which takes into account additional permeabilities (P_{Na}, P_{Cl}). If $E_{Cl} = E_M$, this equation may be simplified to

$$E_M = 58{\cdot}5 \log \frac{[K^+]_o + \alpha[Na^+]_o}{[K^+]_i + \alpha[Na^+]_i},$$

where $\alpha = P_{Na}/P_K$, the ratio of Na to K permeability. Taking 10·4 mM as a reasonable value for $[Na^+]_i$ (Conway, 1957), the Goldman equation is plotted over a range of $\Delta[K^+]_o$, assuming different values of α, in Text-fig. 3. The agreement between the experimentally determined points and those generated by assuming $\alpha = 10^{-3}$ suggests that the resting Na permeability of the neurones is about 1/1000 the K permeability. This result may be compared with those from other nerve cells, for which $\alpha \sim 10^{-2}$ gives the best fit with the experimental results (Huxley & Stämpfli, 1951).

The E_M predicted by the Goldman equation with $[K^+]_o = 0{\cdot}3$ mM and $\alpha = 10^{-3}$ is 9 mV more negative than the observed value of -131 mV. This result would be expected if the effective $[K^+]_o$ during perfusion with 0·3 mM were actually 0·46 mM. Such a value for external K ion concentration might arise if there were only slow equilibration of the low K^+ perfusion solution with the fluid in the extracellular space. Leakage of K^+ from cells damaged during the dissection could contribute to an elevation of its concentration in the vicinity of the neurones. Another alternative is that the membrane permeability to other ions has a significant influence at such large resting potentials.

Resting potentials in muscle cells

Resting potentials of muscle cells were studied in tadpoles at the same developmental stages (NF 45–49), both as a check on technique and for purposes of comparison with Rohon–Beard cells. The resting potential in 4·3 mM-$[K^+]_o$ has a mean value of -80 mV; values in 12·0 and 1·0 are -54 and -117 mV, respectively. In Text-fig. 4, muscle cell resting potential is plotted against the log $[K^+]_o$, and the straight line drawn by eye. The slope of the plot is 58·5 mV per tenfold change in $[K^+]_o$. This value is in good agreement with the predictions of the Nernst equation, and appears not to differ significantly from the results obtained for Rohon–

Beard cells (compare with Text-fig. 2). Confirming the results of Cohen *et al.* (1968), muscle cells also behave like K^+ electrodes over a large range of $[K^+]_o$ concentrations.

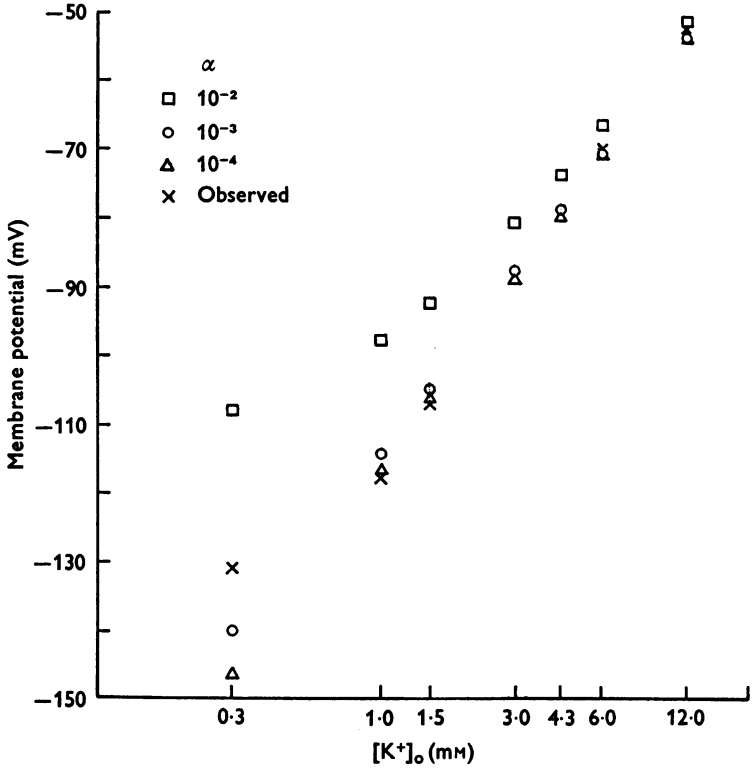

Text-fig. 3. Comparison of experimental determinations of Rohon–Beard resting potentials with predictions of the Goldman equation. Points graphed as in Text-fig. 2. Theoretical plots assume different values of α (P_{Na}/P_K). The best agreement with the observed points is obtained when $\alpha \leqslant 10^{-3}$, indicating $P_{Na} \leqslant P_K/1000$.

Response to stimulation of the spinal cord

Antidromic action potentials

The sensitive dependence of the Rohon–Beard neurones' resting potential on the $[K^+]_o$ could have interesting consequences for their physiological activity in the spinal cord. It seemed likely that increases in $[K^+]_o$, resulting from the efflux of K^+ during action potentials in nearby neurones, would depolarize these cells. To test this hypothesis, experiments were made in which the anterior end of the cord was stimulated with a suction electrode while recording from Rohon–Beard cells. In all these

experiments the Ringer solutions contained 3·0 instead of 4·3 mM $[K^+]_o$, since the response to increases in extracellular K^+ was expected to be larger in low initial $[K^+]_o$. Curare was routinely added to the solutions at 10^{-5} g/ml. to prevent muscle contraction.

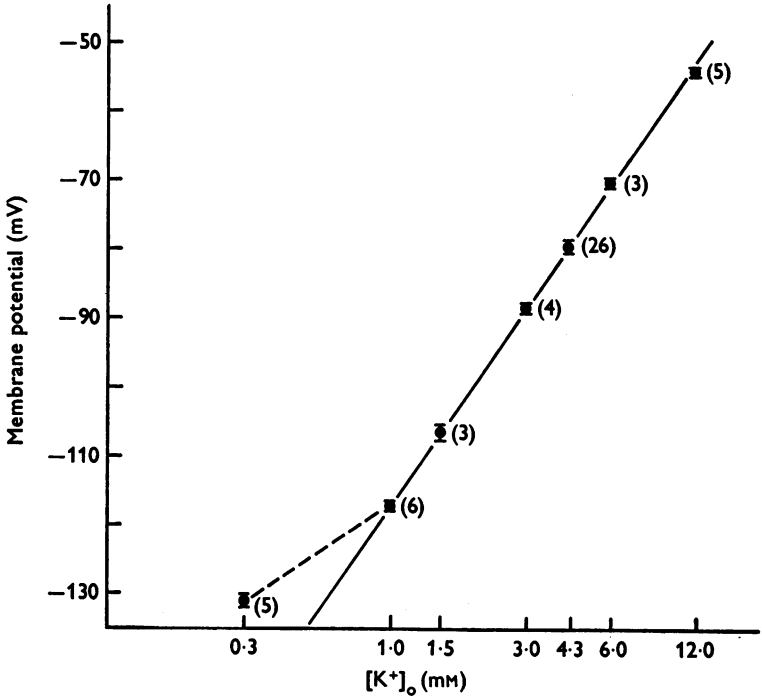

Text-fig. 4. The dependence of muscle cell resting potentials on $[K^+]_o$. Data plotted as in Text-fig. 2, and the lines drawn by eye. The slope of the continuous line is 58·5 mV/10 × $\Delta[K^+]_o$, which is close to that obtained for Rohon–Beard neurones (compare with Text-fig. 2) NF 45–49.

A brief current pulse of either polarity often gave rise to a small potential sufficient to initiate an action potential, as illustrated in Text-fig. 5. Following a latency of 5·2 msec in this case, there is a two-stage response (5*A*); the point of inflexion on the rising phase of the depolarization is clearly indicated by the record of dV/dt. Repeated stimulation at a low frequency (1 Hz) usually led to a decline in the size of the potential sufficient to render it subthreshold for spike initiation. A recording from another Rohon–Beard cell further caudal along the spinal cord first shows prepotential and action potential occurring 9·0 msec after the stimulus, and the response after further trials when the prepotential is subthreshold (5*B*).

It seemed possible that stimulation of the cord was giving rise either to

synaptic potentials which were susceptible to fatigue, or to antidromic spikes which were blocked at increasing distances from the cell body. Collision experiments were carried out to distinguish between these two alternatives, as illustrated in Text-fig. 6. The procedure was to initiate an

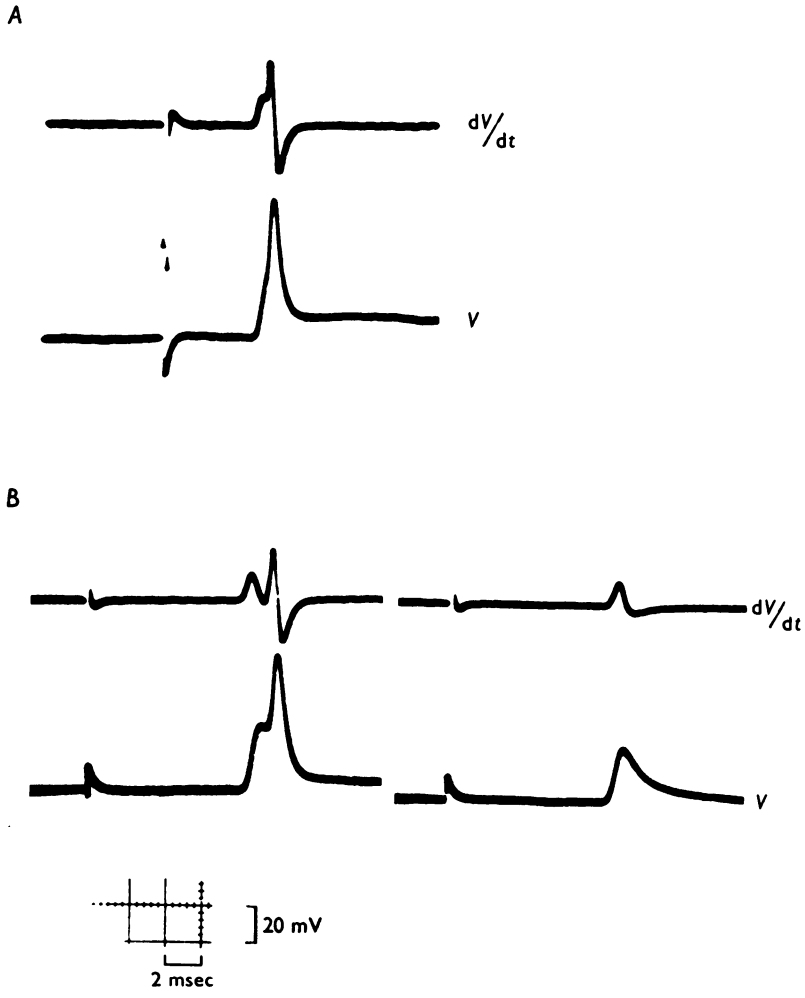

Text-fig. 5. Antidromic action potentials in Rohon–Beard neurones, following stimulation of the anterior end of the spinal cord with a suction electrode. *A*, the invading spike brings the cell to threshold and triggers an action potential in the cell body. The threshold is clearly indicated by the inflexion on the rising phase of the differentiated record. Resting potential −92 (3·0 mM-$[K^+]_o$), NF 47. *B*, in another cell in the same preparation, the antidromic action potential becomes subthreshold upon repeated stimulation. Same 0·05 msec stimulus, reverse polarity; two consecutive trials, 1 sec apart. Resting potential −82 (3·0 mM-$[K^+]_o$).

action potential by passing a depolarizing current pulse through the recording electrode, and determine when cord stimulation was successful in producing a second action potential which could be recorded in the cell body. Conduction time, according to Text-fig. 6*A*, was 9·2 msec. The shortest time, after the first action potential, that cord stimulation

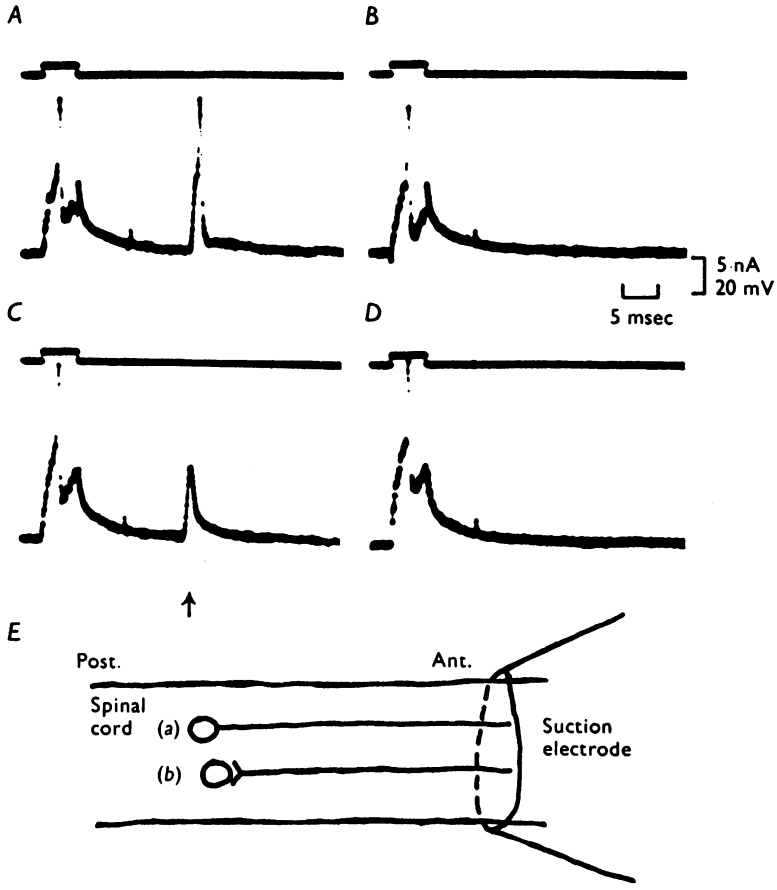

Text-fig. 6. Collision experiment demonstrates that spinal cord stimulation produces antidromic action potentials in Rohon–Beard cells. An action potential in response to intracellularly injected current is followed by stimulation of the anterior end of the cord 6·73 mm distant. *A*, stimulation 10·6 msec after the first spike yields a second spike in the cell body 9·2 msec later. *B*, the second spike is absent when the cord is stimulated 10·3 msec after the first. *C*, later, in the same cell, cord stimulation 10·5 msec after the first action potential produces a second, that is subthreshold for spike initiation in the cell body. *D*, the identity of the antidromic axonal spike (arrow in *C*) is confirmed by its collision with the action potential set up in the cell body. Resting potential −90 (3·0 mM-$[K^+]_o$); NF 47. *E*, the results are most simply explained on the basis of circuitry indicated by (*a*).

evoked a second action potential was never less than 10·5 msec (Text-fig. 6*A*, *B*). The same result was obtained when the antidromic spike was subthreshold for impulse initiation in the cell body (Text-fig. 6*C*, *D*). The simplest interpretation is that the scheme of Text-fig. 6*Ea* applies and that the refractory period in this experiment was about 1·3 msec. The conduction velocity, determined as the ratio of distance to latency, was 0·73 m/sec (range for eleven cells, 0·6–0·8 m/sec).

Stimulation of the cord

Slow depolarizations and their mediation by K^+

The aim was to see the effect of impulses of other neurones on the Rohon–Beard cells; the cells thus had to be inactive. When the cord was sufficiently stimulated with single shocks to eliminate action potentials in Rohon–Beard cells, trains of stimuli produced a slow depolarization in the absence of visible synaptic activity. Such an effect is shown in Text-fig. 7. Single stimuli initially caused an antidromic action potential; upon continued stimulation the spike failed to invade the cell body, diminished in size and finally disappeared. At this point a train of eleven stimuli (200 Hz) were delivered to the anterior end of the spinal cord. There was a slow depolarization of 4 mV amplitude which reached its peak 200 msec after the end of the train, indicated by the stimulus artifact (7 *D*). The half-decay time was 430 msec. The same train of stimuli caused no depolarization when the intracellular electrode was just outside the cell (7 *E*).

The magnitude of this depolarization response varies considerably from preparation to preparation, and from cell to cell within a preparation. The effect of a shorter train of 6 stimuli is seen in Text-fig. 7 *F*. The depolarization commences roughly 30 msec after the end of the train and rises to a peak amplitude of 5·5 mV in 200 msec (half-decay time 380 msec). The largest response observed in these experiments was 9·4 mV to a train of eleven stimuli (7 *G*). In this case the depolarization has its onset during the train and continues to increase by another 3 mV after the end of stimulation; time to peak is 300 msec. The magnitude of the effect in any particular cell is relatively constant from one train to the next, when trains are presented at intervals $\geqslant 30$ sec. After numerous trials the response declined. The cause of the decline may be attributed to failure of the cord to respond to stimulation, since the full value of the resting potential was still recorded.

A slow depolarization in response to a single shock is occasionally observed. In Text-fig. 8 *A*, a brief current pulse causes a 4 mV depolarization. When a pair of stimuli are presented, 5 msec, apart, the response to the first is again 4 mV, but the response to the second is 3 mV (8 *B*);

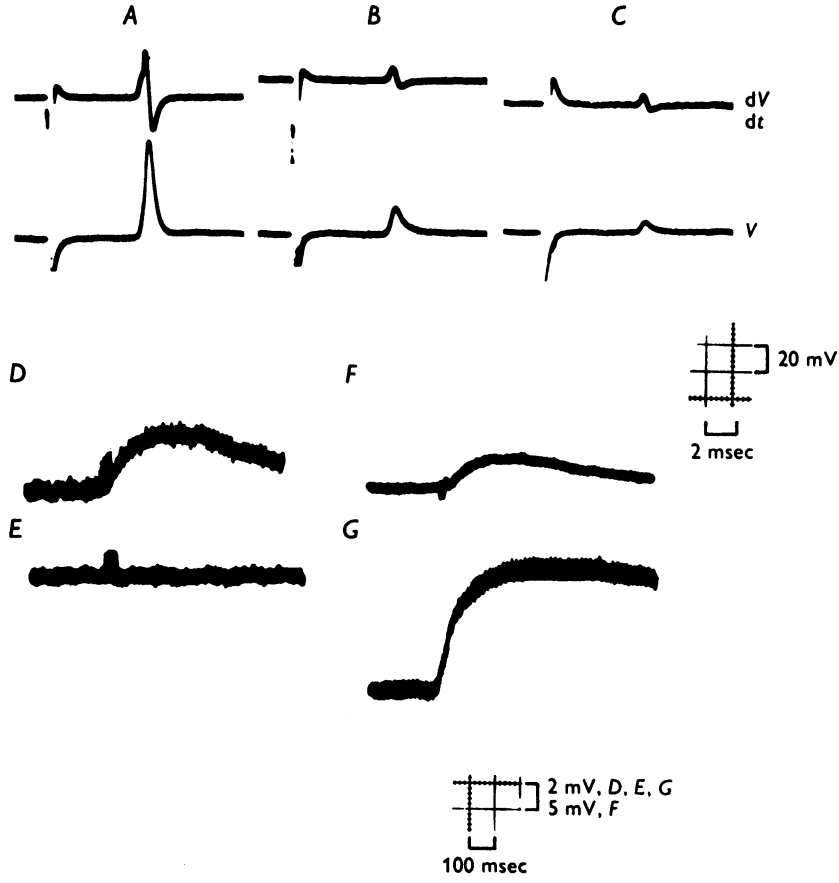

Text-fig. 7. Slow depolarization of Rohon–Beard cell to train of stimuli, in the absence of antidromic activity. *A*, *B*, *C*, responses to 0·2 msec stimulation of the spinal cord, demonstrating progressive block of the antidromic spike. Stimulation at 1 Hz, note increase in gain on d*V*/d*t* records. 0·05 msec stimuli had no effect. *A*, action potential in the cell body; *B*, axonal action potential subthreshold; *C*, axonal spike is further attenuated; *D*, stimulation with train of eleven stimuli (200 Hz, 0·05 msec) yields a 4 mV depolarization which peaks 200 msec after the end of the train. *E*, control, showing absence of response to same train of stimuli when recording electrode withdrawn from cell. All records from same neurone; resting potential −90 (3·0 mM-$[K^+]_o$); NF 48. *F*, train of six stimuli causes 5·5 mV depolarization. Resting potential −86 (3·0 mM-$[K^+]_o$); NF 47. *G*, train of eleven stimuli causes 9·4 mV depolarization. Resting potential −91 (3·0 mM-$[K^+]_o$); NF 48.

Text-figs. 8*C*, *D* show the responses to the same stimuli with the recording electrode outside the cell. The flat traces show that the depolarizations recorded intracellularly are not stimulus artifacts.

The hypothesis that the slow depolarizations of Rohon–Beard neurones are due to K^+ accumulation in their environment can be tested experimentally, using the paradigm employed by Orkand *et al.* (1968) in studying similar responses in leech glial cells. If a standard stimulus causes a response in 3·0 mM-$[K^+]_o$, resulting from the efflux of K^+ from electrically

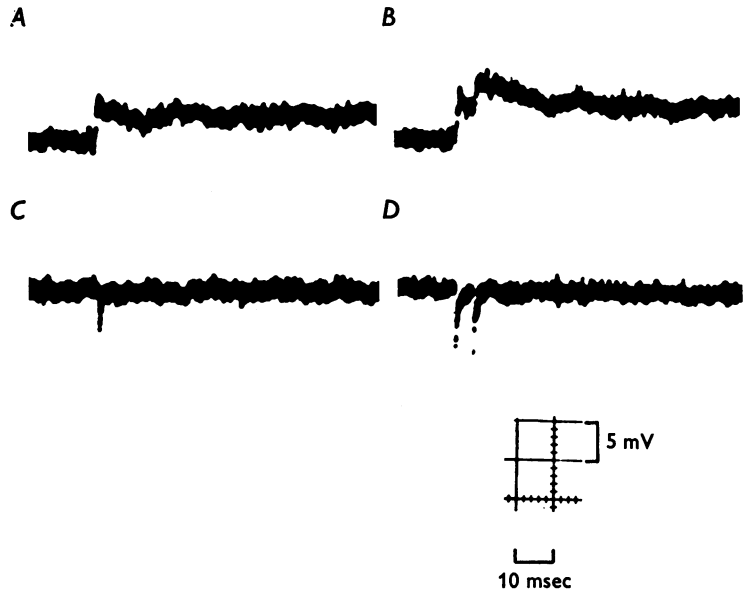

Text-fig. 8. Slow depolarizations to single stimuli given to the anterior end of the spinal cord. *A*, 4 mV response to single shock. *B*, 4 and 3 mV responses to two shocks. Depolarization lasts many tens of msec (note time base); compare with antidromic spike duration (Text-figs. 5, 6 and 7). *C*, *D*, extracellular controls. Resting potential −88 (3·0 mM-$[K^+]_o$); NF 47.

active neurones, a larger response will be expected in 1·5 mM-$[K^+]_o$, and a smaller response in 6·0 mM. Such results are predicted because of the logarithmic dependence of membrane potential on $[K^+]_o$. Furthermore, calculations of the magnitude of the depolarization expected in 1·5 and 6·0 mM-$[K^+]_o$ are possible, knowing the size of the response in 3·0-mM and the relationship established in Text-fig. 2 (resting potential = 59·5 log $[K^+]_o/99$). Accordingly experiments were carried out to examine the size of the response of a Rohon–Beard cell to a constant stimulus, in Ringer with different K^+ concentrations.

Such an experiment is illustrated in Text-fig. 9. A standard train of eleven pulses was given to the anterior end of the spinal cord, while perfusing with solutions containing different concentrations of KCl. Stimulation in 3·0 mM-$[K^+]_o$ produced a 4·9 mV depolarization in this cell.

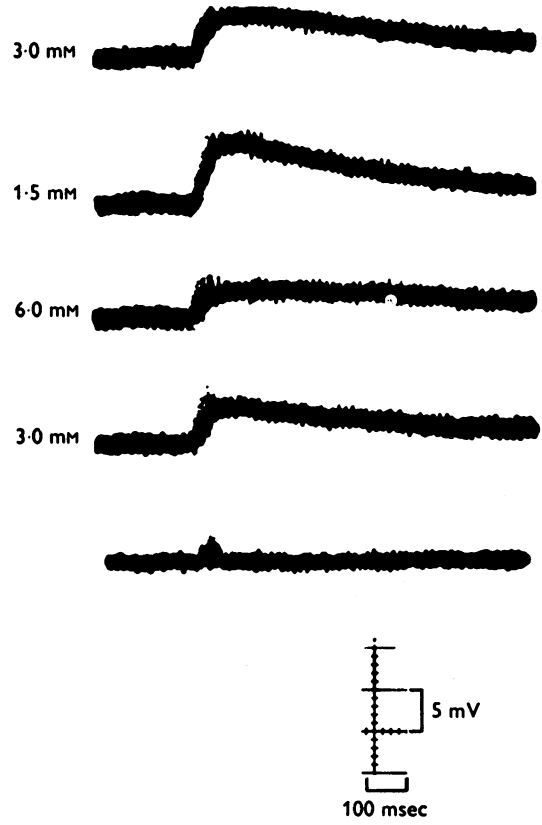

Text-fig. 9. Amplitude of response to train of stimuli in different $[K^+]_o$ solutions. Procedure as in Text-fig. 7. From top: 3·0 mM-$[K^+]_o$ (resting potential −89); 1·5 mM (resting potential −105); 6·0 mM (resting potential −71); 3·0 mM (resting potential −87). Bottom trace, extracellular control. Standard test train of eleven stimuli. The size of the response changes as predicted if the depolarization is due to accumulation of K^+ outside the Rohon–Beard neurone. NF 47.

Stimulation in 1·5 mM yielded 7·8 mV response; in 6·0 mM, 2·8 mV response. Upon return to 3·0 mM, a 4·5 mV response was observed, indicating that the effect is repeatable. The bottom trace indicates the absence of response to stimulation after withdrawal of the intracellular electrode from this neurone.

The increased response in lower $[K^+]_o$ solutions and decreased response in higher $[K^+]_o$ solutions are clearly qualitative changes in the directions predicted by theory. Further, a depolarization of 4·9 mV to stimulation in 3·0 mM-$[K^+]_o$ implies a local increase in $[K^+]_o$ of 0·68 mM. The resting potential expected in 1·5 mM + 0·68 mM would thus be −96·9 mV, and a depolarization of 8·1 mV would be predicted (7·8 mV observed). Similarly, the resting potential expected in 6·0 mM + 0·68 mM would be −68·5, corresponding to a depolarization of 2·5 mV (2·8 mV observed).

This phenomenon has also been analysed in neurones in which attenuated antidromic action potentials were still recorded in response to trains of stimuli. Text-fig. 10*A* illustrates the response of a cell in which the standard train of eleven stimuli produces a series of small antidromic spikes; these appear as a small depolarizing response on a slow time base. However, when the polarity of the stimuli is reversed, they are much more effective in stimulating the cord. The cell membrane has only partially repolarized following the depolarization of summed spikes, when the

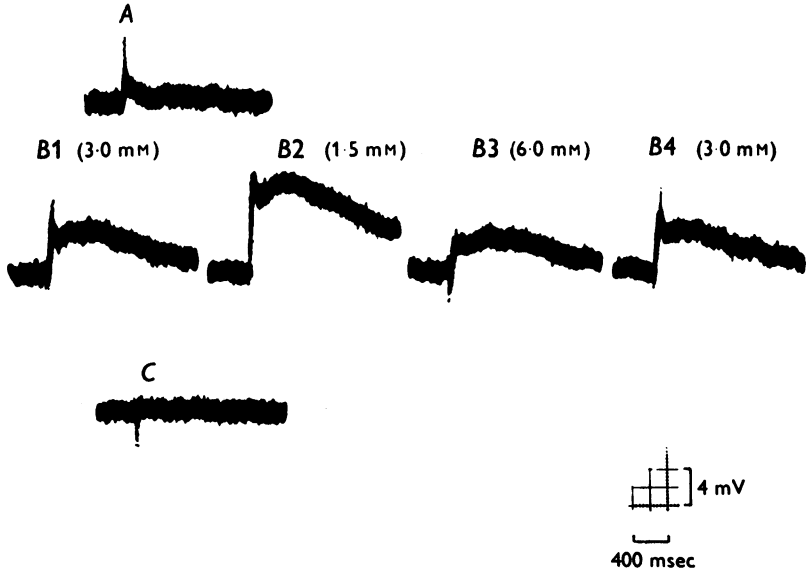

Text-fig. 10. Effect of altering $[K^+]_o$ on size of response to train of stimuli. Procedure as in Text-fig. 7. Each stimulus produces an attenuated spike. *A*, train of eleven pulses gives a train of spikes only. *B*, same train, reverse polarity, gives a train of spikes plus later slow depolarization. 3·0 mM-$[K^+]_o$ (resting potential −88) in *A*, *B*1; 1·5 mM (resting potential −106), *B*2; 6·0 mM (resting potential −71), *B*3; 3·0 mM (resting potential −87), *B*4. *C*, same stimulation as in *B*, recording electrode extracellular. The size of the depolarization in *B* varies as expected by theory when $[K^+]_o$ is changed. Analysis in text. NF 48.

onset of a slow depolarization becomes apparent (10 *B*, 1). In 3·0 mM-$[K^+]_o$ (resting potential −88 mV) this stimulation causes a depolarization of 5·2 mV, with a rise time of roughly 100 msec. A response of this magnitude implies the accumulation of 0·73 mM-$[K^+]_o$.

We may now compare the depolarizations observed in different $[K^+]$ solutions with those predicted on theoretical grounds for this cell. In 1·5 mM-$[K^+]_o$ (resting potential −106) the train of stimuli causes a depolarization of 9·8 mV (10 *B*, 2); a value of 9·6 mV is expected. In 6·0 mM (resting potential −71) stimulation produces a response of 3·0 mV (10 *B*, 3); calculation indicates 2·7 mV depolarization should be observed. When the preparation is again perfused with a solution containing 3·0 mM-$[K^+]_o$ (resting potential −87) a depolarization of 5·0 mV is recorded, which is very close to the initial response. The same stimulus has no effect when the recording electrode is just outside the cell (10*C*).

The calculations from these experiments involve several assumptions. The first is that the stimulation causes the same efflux of K^+ in the $\Delta[K^+]_o$ solutions. Although the potassium conductance, g_K, is probably the same during neuronal repolarization in 6·0 mM-$[K^+]_o$ as in 1·5 mM, the driving force on K^+ (E_M [the membrane potential] $- E_K$) is clearly less in the solution with the higher external K^+ concentration; this assumption is only an approximation. The second assumption is that diffusion of accumulated K^+ out of extracellular space surrounding the Rohon–Beard neurones is not significantly different in $\Delta[K^+]_o$ solutions. Since the maximum $[K^+]_o$ concentration gradient varies by 25%, from 1·5 (in 1·5 mM) to 1·1 (in 6·0 mM; Text-fig. 10) diffusion rates will differ somewhat. Although corrections might be calculated to avoid these assumptions, it may be that the magnitude of any correction lies within the value of experimental error, since there is relatively good agreement of the experimental predictions and the observed results for the six cells studied and analysed as above.

The magnitude of the response to a train of pulses should show logarithmic dependence on the number of stimuli, if all stimuli cause equal K^+ efflux and are closely spaced relative to the decay time of a single response. Evidence in support of this point is presented in Text-fig. 11, showing the responses of a cell to stimulation of the cord with consecutive trains of eleven, nine, seven, five and three pulses. The expected relation between the depolarization and the number of pulses is observed for trains of five to eleven stimuli. This result also provides evidence that at 200 Hz the axons follow the rate of stimulation. The response to three stimuli does not fit this relationship, however, perhaps due to the firing of many axons in response to the initial stimuli, after which they cease to respond to further stimulation.

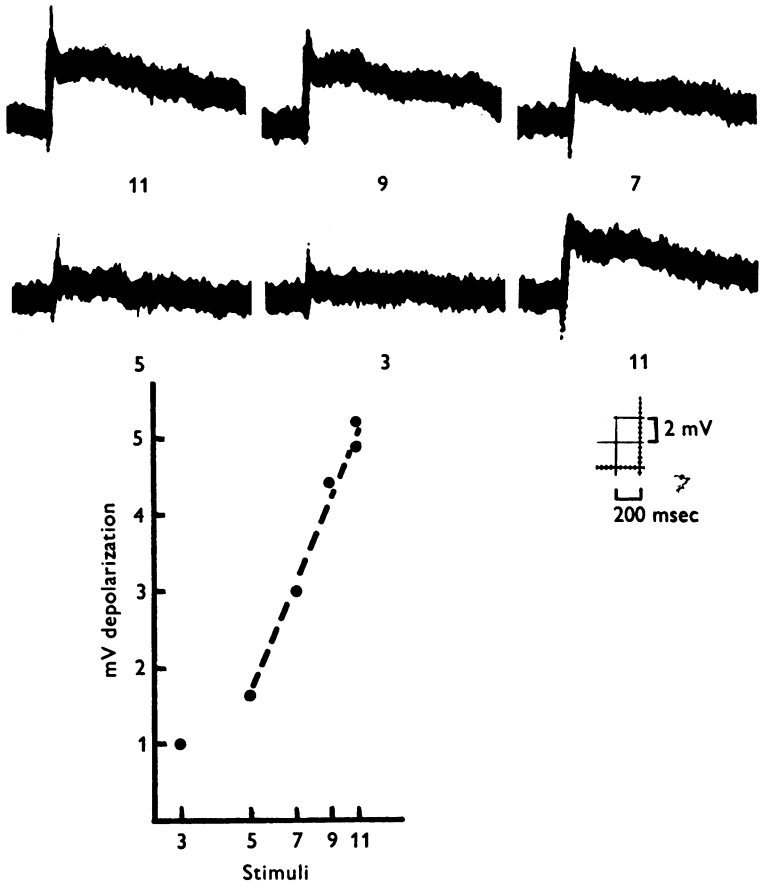

Text-fig. 11. Responses to stimulation with trains of different duration. Eleven, nine, seven, five and three stimuli produce responses of decreasing amplitude; the second response to eleven stimuli is nearly the same as the first. The relationship of mV depolarization to number of stimuli is graphed on the semilogarithmic plot (inset). The points for five to eleven stimuli lie close to the straight line, drawn by eye. Resting potential −91 (3·0 mM), same cell as in Text-fig. 10.

The magnitude of the slow depolarization depends on the frequency of stimulation. In the initial experiments seeking to demonstrate the existence of the slow response, it was observed that a train of eleven stimuli at 200 Hz was more effective than the same number of stimuli at 100 or 50 Hz. This frequency dependence was not further studied.

It is of interest to ask what the necessary and sufficient requirements are to achieve these relatively slow depolarizing shifts of neuronal resting potentials. Are action potentials in Rohon–Beard cells alone an adequate stimulus for this kind of response? A single shock is often effective in

eliciting an action potential, as indicated in Text-fig. 12*A*. This cell was unusual in that a train of sixteen stimuli produced a train of sixteen action potentials (12*B*). The extended electrical activity of this cell depolarized it only by a constant amount, however; no slow, graded depolarization was seen. The stimulus artifacts observed below the continuous trace are the only effects of the train noted after withdrawal of the electrode from the cell.

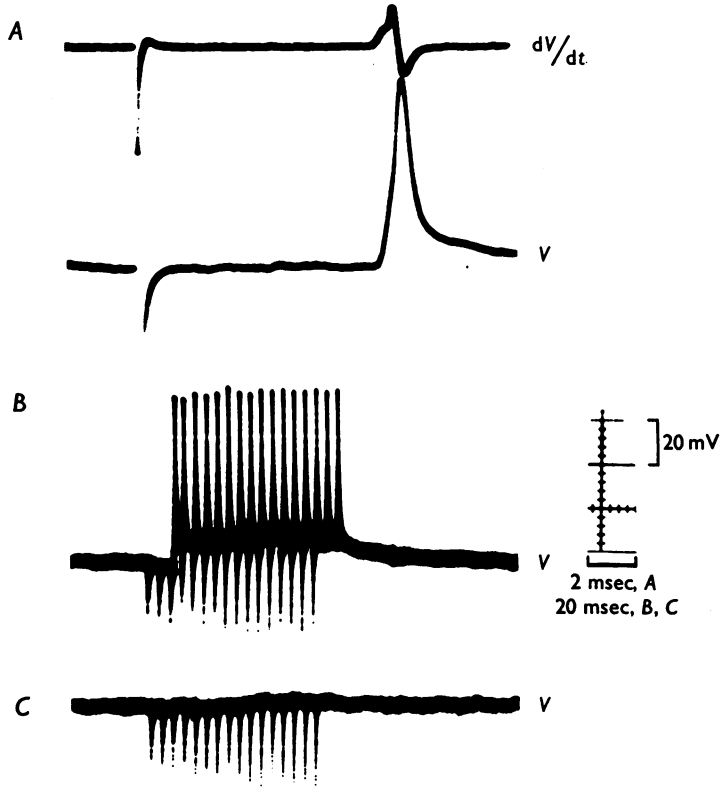

Text-fig. 12. Train of action potentials in Rohon–Beard cell not sufficient to produce slow depolarization. *A*, action potential in response to single stimulus of anterior end of spinal cord. *B*, train of sixteen action potentials; note absence of slow depolarizing shift of resting potential. *C*, same train of stimuli as in *B*, recording electrode extracellular. Resting potential −91 (3·0 mM). NF 48.

This result suggests that the electrical activity of Rohon–Beard cells in these dissected preparations may not be sufficient to produce their slow depolarization; in more intact preparations the results might be different. These depolarizations have also been observed with superimposed action potentials, in response to stimulation with a train, however. It is clear that stimulation of the spinal cord generally gives rise to action potentials in

the cord, as evidenced by the production of antidromic action potentials in Rohon–Beard cells. It seems likely that it is the action potentials in these other neurones that contribute the efflux of K which yields the slow depolarizations reported here.

The evidence presented so far supports the hypothesis that the slow depolarization following a train of stimuli is due to an increase in extracellular $[K^+]$. However, it seemed possible that these responses were the results of the release of a chemical synaptic transmitter, causing a slow conductance change. If this were the case the transmitter should have a reversal potential, and polarization of the cell to different levels might be expected to increase or decrease the response.

A number of experiments were made in which the effect of stimulation of the cord was examined at several cell resting potentials. It was possible to shift the membrane voltage in either direction by passing small currents through the recording electrode. Although it is difficult to be completely confident of bridge balance, especially during the passage of long current pulses, satisfactory recordings were obtained from four cells. No significant change in the magnitude of the response was observed; records from one of these cells are illustrated in Text-fig. 13. A current of 0·4 nA hyperpolarizes the cell by 16 mV, shifting the resting potential from -90 to -106 mV. The response to a standard train of stimuli in the hyperpolarized cell is 7·8 mV. The response to the same stimulation in the absence of polarizing current is 7·2 mV, which is within the range of fluctuation of these potential changes. The hyperpolarization of this cell is equivalent to that seen on perfusion with 1·5 mM-$[K^+]_o$; however, in perfusion with low $[K^+]_o$ one would expect a 12·4 mV response.

If the response involved the release of a synaptic transmitter, low Ca-high Mg Ringer would be expected to abolish it. When the normal solution was replaced with one containing 0·5 mM-$[Ca^{2+}]_o$, 10·0 mM-$[Mg^{2+}]_o$, neuromuscular transmission of the myotomes was fully blocked in 5 min, as judged by the absence of movement of the preparation upon tetanic stimulation of the spinal cord. The slow depolarization of Rohon–Beard cells was observed as much as 20 min after this block of stimulus-evoked transmitter release from motor nerve terminals. It thus seems unlikely that these responses are due to chemical synaptic action.

DISCUSSION

Resting potentials

The results show that Rohon–Beard neurones have a resting potential that varies linearly with the logarithm of the external K^+ concentration over a wide range. The slope of this dependence is 59·5 mV/tenfold change

in $[K^+]_o$ at 22° C, which indicates that the potential is derived entirely from the K^+ concentration gradient across the membrane. Since the resting potential is accurately predicted by the Nernst equation, the cells are at the K equilibrium potential, E_K. These nerve cells thus have a unique property, not previously reported for other neurones; they behave like K^+

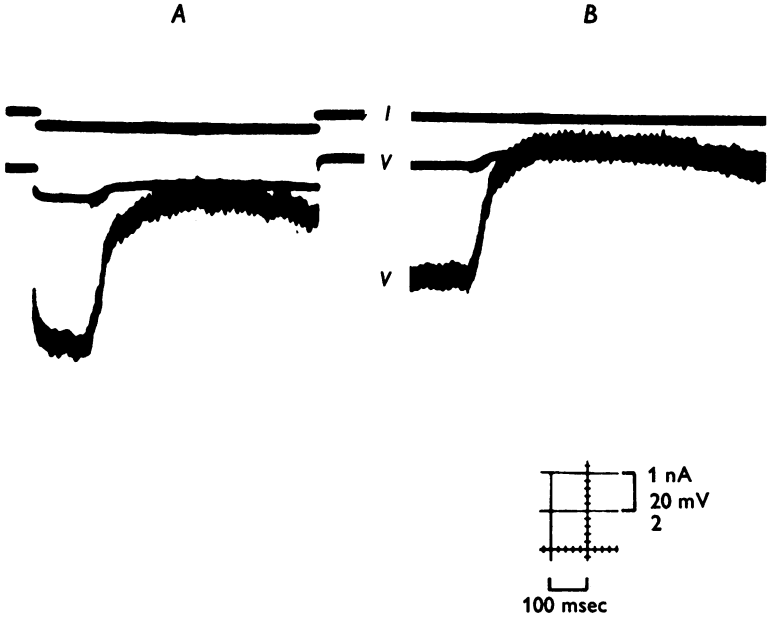

Text-fig. 13. Effect of cell polarization on the response to stimulation of the spinal cord with a train of pulses. Initial procedure as in Text-fig. 7. *A*, cell hyperpolarized by 16 mV with a long current pulse, then cord stimulated with the standard train. *B*, response to same train, in absence of hyperpolarization. The two responses are nearly the same amplitude. Resting potential −91 (3·0 mM). NF 48.

electrodes down to $[K^+]_o$ of 1·0 mM, where the resting potential is −118 mV. Extrapolation of this linear dependence back to 0 mV shows that the cells have an internal concentration of 99 mM-K^+. The strong dependence of the resting potential on K implies a low permeability to other ions, particularly Na. The best fit of the Goldman equation to the observed data is obtained for values of $\alpha \leqslant 10^{-3}$, suggesting that P_{Na} is some three orders of magnitude smaller than P_K. These findings differ from those for other neurones (Huxley & Stämpfli, 1951; Gorman & Marmor, 1974), in which P_{Na} makes an appreciable contribution to the resting potential. The Goldman equation adequately predicts the value of the resting potential for these cells with $\alpha \sim 10^{-2}$.

Glial cells were the first to be observed to have resting potentials at

E_K (Kuffler *et al.* 1966). Subsequently Cohen *et al.* (1968) demonstrated that muscle cells also behave like K^+ electrodes. This result was confirmed in the present study and extended to lower values of $[K^+]_o$. In 1·0 mM-K^+ muscle cells have a resting potential of -117 mV. There seems to be no significant difference between the $[K^+]_o$ dependence of Rohon–Beard neurone and muscle cell resting potentials.

The mean values for the resting potential at each of seven different external K^+ concentrations lie very close to the straight line fitted to them, and standard errors are small. Only one third of cells examined satisfied the stringent criteria for acceptance of the recorded value (see Methods), in 6·0 and 12·0 mM-$[K^+]_o$. Only one sixth of cells met the criteria in low $[K^+]_o$ solutions (1·0 and 0·3 mM), where the driving force on Na^+ through any leak conductance was greater. If these standards for the selection of data are relaxed, there is more scatter in the values and the means lie above the straight line.

The observation of such large resting potentials in these neurones at NF 45–49 prompts one to ask when the membrane first acquires its low α. The resting potential of fertilized *Xenopus* eggs is -6 mV; it is -57 mV in blastulae, NF 9 (0·7 mM-$[K^+]_o$) (Palmer & Slack, 1970; Slack, Warner & Warren, 1973). The new membrane appearing at the time of first cleavage has a much lower specific resistance and a different ionic permeability that than of the egg (deLaat & Bluemink, 1974). The birthdate of a population of neurones has been defined by Sidman (1970) as the time of the final round of DNA synthesis by their precursor cells. Rohon–Beard cells have been birthdated at stage NF 12 (Spitzer & Spitzer, 1975). Recordings have been made from embryos as early as stage NF 26 (30 hr old), and the resting potential in Rohon–Beard cells is -80 mV (4·3 mM K^+) (unpublished observation). This value is not significantly different from that in older animals. It seems likely that these neurones already have their mature resting membrane characteristics by this time. The Rohon–Beard cells in *Xenopus* tadpoles can no longer be found after 4 weeks (NF 55) (Hughes, 1957), and presumably have died (Nieuwkoop & Faber, 1956). It will be of interest to see if there is any change in their resting membrane properties before the time they disappear.

Is the dependence of the resting potential on the potassium ion concentration gradient an exclusive characteristic of Rohon–Beard cells, or the property of a more general class of vertebrate neurones? Dorsal root ganglion cells at NF 49–50 have -90 mV potentials in 3·0 mM-$[K^+]_o$ (P. Baccaglini, personal communication). Dorsal root ganglia, like Rohon–Beard neurones, and glia, are derived from the neural crest (DuShane, 1938). It seems possible that it is sensory neurones or neural crest derivatives generally that have large membrane potentials in the tadpoles.

Another alternative is that all neurones have this property in larval amphibians. On this view one might expect interneurones (e.g. Mauthner cells) and motor neurones to have equally large resting potentials. Historically, the resting potentials of nerve cells may appear to increase as higher resistance micro-electrodes with finer tips are employed, and the damage produced by impalement decreases. Cells with resting potentials at E_K may be more common than presently recognized. A number of nerve cell lines in tissue culture exhibit large resting potentials. Fischbach & Dichter (1974) observed values of -74 mV ($\sim 5{\cdot}4$ mM-$[K^+]_o$) in neurones dissociated from embryonic chick spinal cords. O'Lague, Obata, Claude, Furshpan & Potter (1974) recorded -70 mV ($5{\cdot}5$ mM-$[K^+]_o$) potentials in mouse embryo superior cervical ganglion cells in culture. Dennis, Harris & Kuffler (1971) observed resting potentials of -75 mV or more ($4{\cdot}6$ mM-$[K^+]_o$) in parasympathetic neurones in the heart of adult toads (*Bufo marinus*) and frogs (*R. catesbiana*). Some of these values are a few millivolts more positive than those reported here, but the internal K^+ concentration in these cells is not known. The dorsal cells of the adult sea lamprey have resting potentials of only -70 mV ($2{\cdot}1$ mM-$[K^+]_o$) (Martin & Wickelgren, 1971). These cells may be homologous to Rohon–Beard neurones; since their internal K^+ concentration has not been determined, it is not known if this resting potential is at E_K.

Other cell properties

Rohon–Beard neurones have an input resistance of about 40 MΩ. No significant changes have been noted as embryos develop from NF 45 to NF 49. This value is close to those observed by Dennis *et al.* (1971) in adult amphibian parasympathetic neurones (20–50 MΩ).

Although the action potential has a conventional appearance, there is no undershoot when it is triggered after the termination of a brief depolarizing current pulse. The undershoot is a result of the high g_K during the repolarization phase, driving the cell toward E_K, which for many neurones is more negative than the resting potential. The absence of any hyperpolarization following the spike confirms that these cells have their resting potential at E_K. When cells are depolarized by current pulses that outlast the action potential, the passive depolarization of the cell displaces the membrane potential far enough from E_K for an undershoot to be developed.

The observation of antidromic action potentials in Rohon–Beard neurones is parallel to similar observations on dorsal cells in the lamprey (Rovainen, 1967; Martin & Wickelgren, 1971). The conduction velocity of $0{\cdot}75$ m/sec at 22° C is comparable to that measured by Rovainen for dorsal cells ($0{\cdot}4$ m/sec at 6–10° C). The shape of the antidromic spike when it is

blocked at some distance from the cell body resembles that of a post-synaptic potential (Text-fig. 5 *B*), as previously observed in other neurones (Eccles, 1957; Varon & Raiborn, 1971; Bunge, Rees, Wood, Burton & Ko, 1974).

Slow depolarization

In the absence of obvious antidromic or synaptic activity, trains of stimuli often cause a much slower depolarization of Rohon–Beard neurones. Less frequently, a single stimulus produces the same kind of effect. This response is usually repeatable, provided that the frequency of trials is no greater than 2–3/min. The phenomenon is likely to be due to the accumulation of K^+ in the extracellular space surrounding the cells, as a result of the electrical activity of other neurones in the spinal cord. A number of lines of evidence support this contention. The most significant is that the magnitude of the depolarization depends on the amount of K^+ already present. This dependence can be predicted because of the logarithmic relation between K^+_o concentration and membrane potential, as first demonstrated for glia cells by Orkand *et al.* (1966). The agreement of the theoretical predictions with the observed results strongly suggests that the depolarization is due to the build-up of $[K^+]$ in their environment. A second point in favour of this interpretation is the observation that the size of the response is independent of the membrane potential, *per se*. Cells can be hyperpolarized or depolarized with injected currents without appreciably altering the size of the response. Such a result argues against a p.s.p. produced by a chemical transmitter, with a standard reversal potential. Further, calculations show that the magnitude of the slow depolarizations in three different $[K^+]_o$ solutions (e.g. Text-fig. 10) cannot be simply explained by a conductance change with a single equilibrium potential. Thirdly, this response is not eliminated by low Ca^{2+}, high Mg^{2+} concentrations that block transmission at chemical synapses. Fourthly, the graded nature of the response is in agreement with the expectation that an equal amount of K^+ is released by each stimulus. Finally, the time course of the potential change is consistent with what might be expected on the basis of accumulation and disappearance of a substance by diffusion. The depolarization starts during or after a train of stimuli, presumably depending on the proximity of activated nerve cells acting as a source of K^+. The peak depolarization is reached in 50–300 msec after the end of a train of stimuli and may take more than a second to decay (e.g. Text-fig. 10), values comparable to those obtained in other preparations.

The largest depolarization seen in this study is 9 mV in 3·0 mM-$[K^+]_o$, corresponding to a final K^+ concentration of 4·3 mM. This is much smaller

than the 48 mV reported by Orkand *et al.* (1966) in glia of *Necturus* optic nerve, equivalent to a peak concentration of 20 mM, even though the frequency of stimulation (200 Hz) is 20 × that necessary to give the maximum depolarization of glia. Baylor & Nicholls (1969*a*) also observed a larger increase in $[K^+]_o$ (3 mM) around leech neurones in response to lower frequencies of stimulation (45 Hz) than those used here. The investigation of Kríz, Syková, Ujec & Vyklický (1974) is particularly relevant to this study. Stimulation at 100 Hz of afferents to the cat spinal cord caused a local increase in $[K^+]_o$ of 3 mM, measured at a depth of 1·4 mm in the cord. It seems likely that the accumulation of K^+ in the preparations studied here is small because of the extensive dissection, and the superficial location of Rohon–Beard cells in the spinal cord. The effect noted by Baylor & Nicholls was abolished by removal of the surrounding glia. It is perhaps remarkable that depolarizations as large as those reported here can be obtained in such radically dissected preparation under conditions of continuous perfusion. It is not known if the stimulation rate used in this study (200 Hz) is in the physiological range; larger responses might be obtained with lower stimulation frequencies from more intact animals.

The magnitude of the response has a strong dependence on the initial extracellular concentration of K^+, because of the logarithmic relation of $[K^+]_o$ to membrane potential. For this reason it is important to know the concentration *in vivo*. No measurements were made on these embryos, but Conway (1957) reported a value of 2·15 mM-$[K^+]_o$ for adult frog plasma. A value of 1·1 mM has been obtained more recently for *Xenopus* embryos at NF 1–9 (Slack *et al.* 1973). These results imply that Rohon–Beard neurones have a resting membrane potential in the neighbourhood of −98 to −115 mV *in vivo*, and are highly sensitive to small increases in $[K^+]_o$ around them.

What is the source of K^+ that causes these responses in dissected preparations? Trains of action potentials in Rohon–Beard cells are not necessary for the accumulation of K^+ around them, although slow depolarizations have been observed with superimposed spikes. In some instances (Text-fig. 12), action potentials in Rohon–Beard cells were not sufficient to cause a depolarization in these dissected preparations. The impulse activity of other neurones in the spinal cord contribute the efflux of K^+ producing the response. There is no information about the number of other nerve cell processes that surround the Rohon–Beard neurones, and how many of these are active when the cord is stimulated. These considerations make it impossible to calculate the release of K^+/cm^2 of axon from the results given here, although it is likely to be the same as that of other preparations (Baylor & Nicholls, 1969*a*; Keynes & Ritchie, 1965).

In contrast, increases in extracellular $[K^+]$ in the intact animal could

result from activity of the Rohon–Beard cells themselves, or that of other neurones in the spinal cord. The skin cells of *Xenopus* embryos have been shown to conduct action potentials at stages NF 22–41 (Roberts, 1971); it is possible that the repolarization of these cells in the periphery produces an efflux of K^+ sufficient to depolarize Rohon–Beard dendrites.

Dorsal root potentials have been recorded both extra and intracellularly in the spinal cord following stimulation of peripheral nerves. Barron & Matthews (1938) first suggested that they arose from the accumulation of ions around the afferent terminal fibres. The size and time course of these potentials are comparable to those reported here. This phenomenon has been studied recently by several groups of investigators; direct measurements of extracellular $[K^+]$, with K sensitive electrodes, have been compared to the size of the slow, potential changes. The agreement is good in some instances (Krnjević & Morris, 1972; Vyklický, Syková, Kríz & Ujec, 1972), but lacking in others (Somjen & Lothman, 1974).

It is of interest to speculate what the effect of local increases in $[K^+]_o$ may be on the function of these sensory cells. Any shift of the membrane potential in a depolarizing direction should decrease the distance to threshold, so that a smaller generator potential is effective in firing a cell. Accordingly one might expect to observe changes in the receptive field characteristics of Rohon–Beard cells. It is not known if the processes of these cells are gathered in bundles, surrounded by a glial sheath; if they are, the activity of one neurone could increase the sensitivity of other functionally related neurones. Baylor & Nicholls (1969*b*) observed that leech neurones that have just produced an impulse are hyperpolarized and have become more sensitive to K^+ from adjacent cells. In contrast, the Rohon–Beard cells do not increase their sensitivity by hyperpolarization, but could be made more likely to fire as a result of past activity.

It is possible that the electrical activity of various elements in intact animals is sufficient to cause an efflux of K^+ which depolarizes the cells to threshold, causing them to fire. Threshold lies at about -55 mV (Text-figs. 5, 6 and 7), which suggests that a concentration of 12 mM would be adequate, in the absence of membrane rectification. Concentrations of K^+ as high as 20 mM have been observed in *Necturus* optic nerve (Orkand *et al.* 1966), although stimulation of afferents to the cat spinal cord gave concentrations of only 6 mM (Kríz *et al.* 1974).

This work was supported by USPHS grant R01 NS 11311 and a grant from the Alfred P. Sloan Foundation. The author is a Sloan Research Fellow. Henry Kistler provided valuable assistance.

REFERENCES

BARRON, D. H. & MATTHEWS, B. H. C. (1938). The interpretation of potential changes in the spinal cord. *J. Physiol.* **92**, 276–321.

BAYLOR, D. A. & NICHOLLS, J. A. (1969*a*). Changes in extracellular potassium concentration produced by neuronal activity in the central nervous system of the leech. *J. Physiol.* **203**, 555–569.

BAYLOR, D. A. & NICHOLLS, J. G. (1969*b*). After-effects of nerve impulses on signalling in the central nervous system of the leech. *J. Physiol.* **203**, 571–589.

BEARD, J. (1889). On the early development of *Lepidosteus osseus*. *Proc. R. Soc.* **46**, 108–118.

BUNGE, R. P., REES, R., WOOD, P., BURTON, H. & KO, C. (1974). Anatomical and physiological observations on synapses formed on isolated autonomic neurons in tissue culture. *Brain Res.* **66**, 401–412.

COGHILL, G. E. (1914). Correlated anatomical and physiological studies of the growth of the nervous system of amphibia. I. The afferent system of the trunk of *Amblystoma*. *J. comp. Neurol.* **24**, 161–234.

COHEN, M. W., GERSCHENFELD, H. M. & KUFFLER, S. W. (1968). Ionic environment of neurones and glial cells in the brain of an amphibian. *J. Physiol.* **197**, 363–380.

CONWAY, E. J. (1957). Nature and significance of concentration relations of potassium and sodium ions in skeletal muscle. *Physiol. Rev.* **37**, 84–132.

DELAAT, S. W. & BLUEMINK, J. G. (1974). New membrane formation during cytokinesis in normal and cytochalasin B-treated eggs of *Xenopus laevis*. II. Electrophysiological observations *J. cell Biol.* **60**, 529–540.

DENNIS, M. J., HARRIS, A. J. & KUFFLER, S. W. (1971). Synaptic transmission and its duplication by focally applied acetylcholine in parasympathetic neurones in the heart of the frog. *Proc. R. Soc.* B **177**, 509–539.

DUSHANE, G. P. (1938). Neural fold derivatives in the amphibia: pigment cells, spinal ganglia and Rohon-Beard cells. *J. exp. Zool.* **78**, 485–503.

ECCLES, J. C. (1957). *The Physiology of Nerve Cells*. London: Oxford University Press.

FISCHBACH, G. D. & DICHTER, M. A. (1974). Electrophysiologic and morphologic properties of neurons in dissociated chick spinal cord cell cultures. *Devl Biol.* **37**, 100–116.

FRANKENHAEUSER, B. & HODGKIN, A. L. (1956). The after-effects of impulses in the giant fibres of *Loligo*. *J. Physiol.* **131**, 341–376.

FREUD, S. (1877). Über den Ursprung der hinteren Nervenwurzeln in Rückenmark von Ammocoetes. *Sber. Akad. Wiss. Wien* (Abt. 3) **75**, 15–27.

GORMAN, A. L. F. & MARMOR, M. F. (1974). Steady-state contribution of the sodium pump to the resting potential of a molluscan neurone. *J. Physiol.* **242**, 35–48.

HUGHES, A. (1957). The development of the primary sensory system in *Xenopus laevis* (Daudin). *J. Anat.* **91**, 323–338.

HUXLEY, A. F. & STÄMPFLI, R. (1951). Effect of potassium and sodium on resting and action potentials of single myelinated nerve fibres. *J. Physiol.* **112**, 496–508.

KERNAN, P. (1960). Resting potentials in isolated frog sartorius fibres at low external potassium concentrations. *Nature, Lond.* **185**, 471.

KEYNES, R. D. & RITCHIE, J. M. (1965). The movements of labelled ions in mammalian non-myelinated nerve fibres. *J. Physiol.* **179**, 333–367.

KŘÍZ, N., SYKOVÁ, E., UJEC, E. & VYKLICKÝ, L. (1974). Changes of extracellular potassium concentration induced by neuronal activity in the spinal cord of the cat. *J. Physiol.* **238**, 1–15.

KRNJEVIĆ, K. & MORRIS, M. E. (1972). Extracellular K^+ activity and slow potential changes in spinal cord and medulla. *Can. J. Physiol. Pharmacol.* **50**, 1214–1217.

KUFFLER, S. W., NICHOLLS, J. A. & ORKAND, R. K. (1966). Physiological properties of glial cells in the central nervous system of amphibia. *J. Neurophysiol.* **29**, 768–787.

MCMAHAN, U. J. & KUFFLER, S. W. (1971). Visual identification of synaptic boutons on living ganglion cells and of varicosities in postganglionic axons in the heart of the frog. *Proc. R. Soc.* B. **177**, 485–508.

MARTIN, A. R. & WICKELGREN, W. O. (1971). Sensory cells in the spinal cord of the sea lamprey. *J. Physiol.* **212**, 65–83.

NIEUWKOOP, P. D. & FABER, J. (1956). *Normal Table of* Xenopus laevis (*Daudin*). Amsterdam: North Holland Publishing.

O'LAGUE, P. H., OBATA, K., CLAUDE, P., FURSHPAN, E. J. & POTTER, D. D. (1974). Evidence for cholinergic synapses between dissociated rat sympathetic neurons in cell culture. *Proc. natn. Acad. Sci. U.S.A.* **71**, 3602–3606.

ORKAND, R. K., NICHOLLS, J. G. & KUFFLER, S. W. (1966). Effect of nerve impulses on the membrane potential of glial cells in the central nervous system of amphibia. *J. Neurophysiol.* **29**, 788–806.

PALMER, J. F. & SLACK, C. (1970). Some bio-electric parameters of early *Xenopus* embryos. *J. Embryol. exp. Morph.* **24**, 535–553.

ROBERTS, A. (1971). The role of propagated skin impulses in the sensory system of young tadpoles. *Z. vergl. Physiol.* **75**, 388–401.

ROHON, V. (1885). Zur Histogenese des Rückenmarkes der Forelle. *Sber. bayer Akad. Wiss. Math.* (Phys. Kl. Jahrg. 1884) **14**, 39–57.

ROVAINEN, C. M. (1967). Physiological and anatomical studies on large neurons of central nervous system of the sea lamprey (*Petromyzon marinus*). II. Dorsal cells and giant interneurons. *J. Neurophysiol.* **30**, 1024–1042.

SIDMAN, R. L. (1970). Autoradiographic methods and principles for study of the nervous system with H-thymidine. In *Contemporary Research Methods in Neuroanatomy*, ed. NAUTA, J. H. & EBBESON, S. O. E. Berlin and New York: Springer-Verlag.

SLACK, C. & WARNER, A. E. (1973). Intracellular potentials in the early amphibian embryo. *J. Physiol.* **232**, 313–330.

SLACK, C., WARNER, A. E. & WARREN, R. L. (1973). The distribution of sodium and potassium in amphibian embryos during early development. *J. Physiol.* **232**, 297–312.

SOMJEN, G. G. & LOTHMAN, E. W. (1974). Potassium, sustained focal potential shifts, and dorsal root potentials of the mammalian spinal cord. *Brain Res.* **69**, 153–157.

SPITZER, J. L. & SPITZER, N. C. (1975). Time of origin of Rohon-Beard neurons in spinal cord of *Xenopus laevis*. *Am. Zool.* **15**, 781.

VARON, S. & RAIBORN, C. (1971). Excitability and conduction in neurons of dissociated ganglionic cell cultures. *Brain Res.* **30**, 83–98.

VYKLICKÝ, L., SYKOVÁ, E., KŘÍZ, N. & UJEC, E. (1972). Post-stimulation changes of extracellular potassium concentration in the spinal cord of the rat. *Brain Res.* **45**, 608–611.

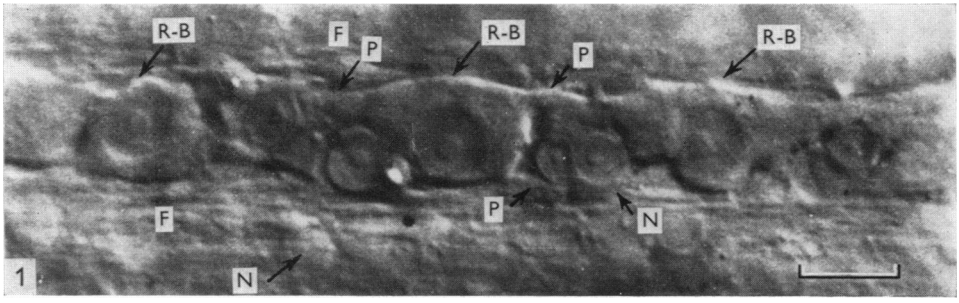

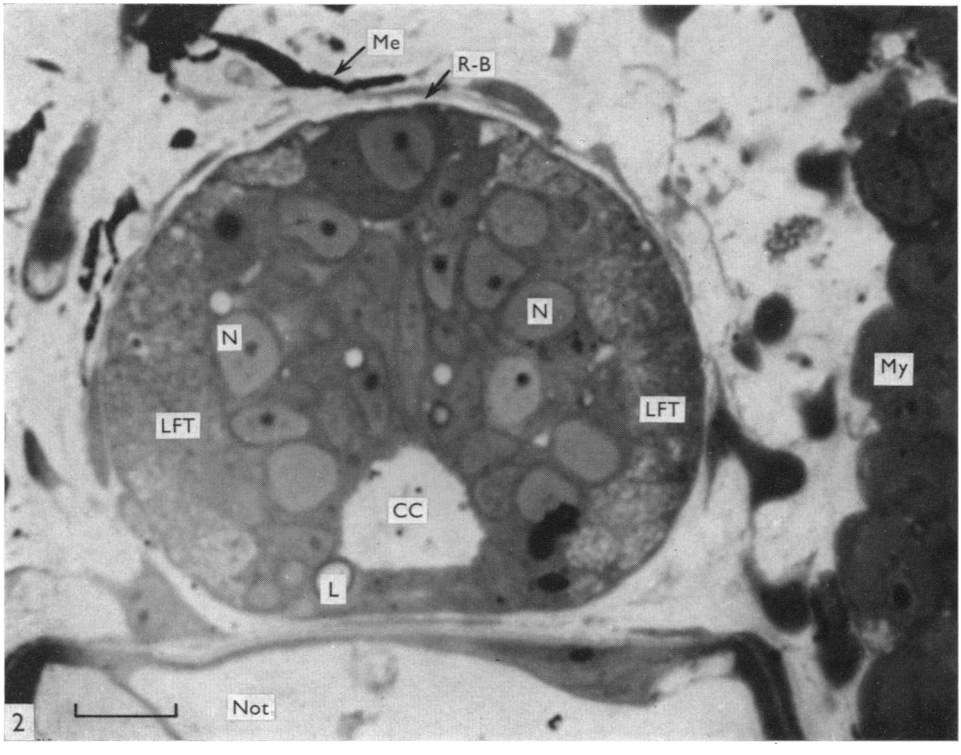

(*Facing p.* 135)

EXPLANATION OF PLATE

The following abbreviations are used: CC, central canal; F, superficial fibres; LFT, lateral fibre tract; L, lipid; Me, melanocyte; My, myotome; N, other neurones; Not, notochord; P, Rohon–Beard cell processes; R-B, Rohon–Beard neurones.

Fig. 1. Nomarski interference contrast micrograph of the surface of the spinal cord of a stage NF 48 tadpole in a dissected preparation, with three Rohon–Beard cells visible in the mid line. The nucleus and prominent nucleolus of these cells are clearly seen. Other, smaller neurones can be discerned, adjacent to Rohon–Beard cells, and deeper in the cord. The processes of cells course along the surface, on either side of the cord. Calibration bar is 20 μm.

Fig. 2. Light microscope picture of a spinal cord (NF 42 tadpole) in cross-section, viewed with bright field optics. Note Rohon–Beard neurone at the dorsal surface of the cord. Yolk and lipid inclusions make it harder to see the Rohon–Beard cells in the fresh preparation. Specimen fixed in phosphate-buffered OsO_4. Calibration 20 μm.